Redox Biology 26 (2019) 101233

Contents lists available at ScienceDirect

Redox Biology

journal homepage: www.elsevier.com/locate/redox

Hippo kinases regulate cell junctions to inhibit tumor metastasis in response to oxidative stress

Yang Wang[a,1], Juan Li[a,1], Ya Gao[a], Yue Luo[a], Hong Luo[a], Liang Wang[a], Yong Yi[a], Zengqiang Yuan[b], Zhi-Xiong Jim Xiao[a,c,*]

[a] Center of Growth, Metabolism and Aging, Key Laboratory of Bio-Resource and Eco-Environment, Ministry of Education, College of Life Sciences, Sichuan University, Chengdu, 610064, China
[b] Institute of Basic Medical Sciences, AMMS, Beijing, 100850, China
[c] Department of Biochemistry, Boston University School of Medicine, Boston, MA, 02118, USA

ARTICLE INFO

Keywords:
Hippo kinase
Metastasis
Δ
Np63α
Cell-cell junction
Cell-matrix adhesion

ABSTRACT

Reactive oxygen species (ROS) are key regulators in cell proliferation, survival, tumor initiation and development. However, the role of ROS in tumor metastasis is less clear. Here, we show that oxidative stress inhibited tumor metastasis via activation of Hippo kinase MST1/2, which led to the phosphorylation and nuclear accumulation of FoxO3a, resulting in upregulation of ΔNp63α expression and suppression of cell migration independent of YAP. Strikingly, while loss of MST1 led to and disruption of cell-cell junction exemplified by reduced E-cadherin expression, resulting in scattered cell growth, loss of MST2 led to disruption of cell-matrix adhesion as evidenced by reduced integrin β4, resulting in increased cell migration and tumor metastasis. Furthermore, expression of MST1 and MST2 was down-regulated in human breast carcinoma. Furthermore, oxidative stress inhibited HER2-or PI3K-mediated tumor metastasis via the MST2-FoxO3a-ΔNp63α pathway. Together, these results that this noncanonical Hippo MST2-FoxO3a-ΔNp63α pathway may play a critical role in ROS-mediated regulation of cell migration and tumor metastasis.

1. Introduction

Tumor metastasis is the main cause of cancer-related death. During metastasis, cancer cells acquire specific traits, including increased migration, invasion, and survival in the bloodstream [1]. Mounting evidence suggests that oxidative stress acts as a key signaling in regulating of tumor initiation, progression and metastasis [2]. Oxidative stress refers to elevated intracellular levels of ROS, which include hydrogen peroxide (H_2O_2), superoxide (O^{2-}) and hydroxyl (OH^-) free radicals [3]. The role of ROS in cancer development is complex as moderate ROS levels have been shown to promote cell proliferation and migration therefore contributing to tumor development [2], while excessive ROS or persistent oxidative stress can cause oxidative damage to lipids, proteins and DNA, eventually leading to apoptosis and senescence to prevent tumor development [4,5]. However, the role of ROS in tumor metastasis remains largely unclear. A recent study reported that ROS can limit distant metastasis and only cells with increased antioxidant capacity can metastasize [6].

Hippo/MST cascade has been well established as a tumor suppressing pathway in the regulation of diverse biologic processes, including cell growth, survival, organ size control and immune response [7–10]. In the canonical pathway, activation of serine/threonine kinases MST1/2 leads to the phosphorylation and activation of their direct substrates, Lats1/2, which in turn phosphorylates and inhibits YAP/TAZ transcription coactivators [11]. Oxidative stress activates MST1, promoting the phosphorylation and nuclear localization of FoxO3, which then transactivates genes involved in apoptotic programs [12,13].

p63 is a member of the tumor suppressor p53 family, and ΔNp63α is the predominant p63 isoform expressed in epithelia cells and is essential for epithelial development [14]. Mounting evidence indicates that ΔNp63α can promote cell proliferation and inhibit oxidative stress-induced cell death [15,16]. On the other hand, ΔNp63α has been documented as an critical metastasis suppressor [17]. ΔNp63α transactivates expression of a subset of genes involved in cell-cell and cell-matrix adhesion, including integrins, E-cadherin, desmoplakin, Par3 and fibronectin [18]. Oncogenic proteins, including activated Ras, PI3K and Her2, can inhibit the expression of ΔNp63α via FoxO3a [19]. Loss of

* Corresponding author. College of Life Sciences, Sichuan University, Chengdu, 610064, China.
E-mail addresses: jimzx@scu.edu.cn, jxiao@bu.edu (Z.-X. Jim Xiao).
[1] Equal contribution.

https://doi.org/10.1016/j.redox.2019.101233
Received 20 March 2019; Received in revised form 22 May 2019; Accepted 31 May 2019
Available online 04 June 2019
2213-2317/ © 2019 The Authors. Published by Elsevier B.V. This is an open access article under the CC BY-NC-ND license (http://creativecommons.org/licenses/BY-NC-ND/4.0/).

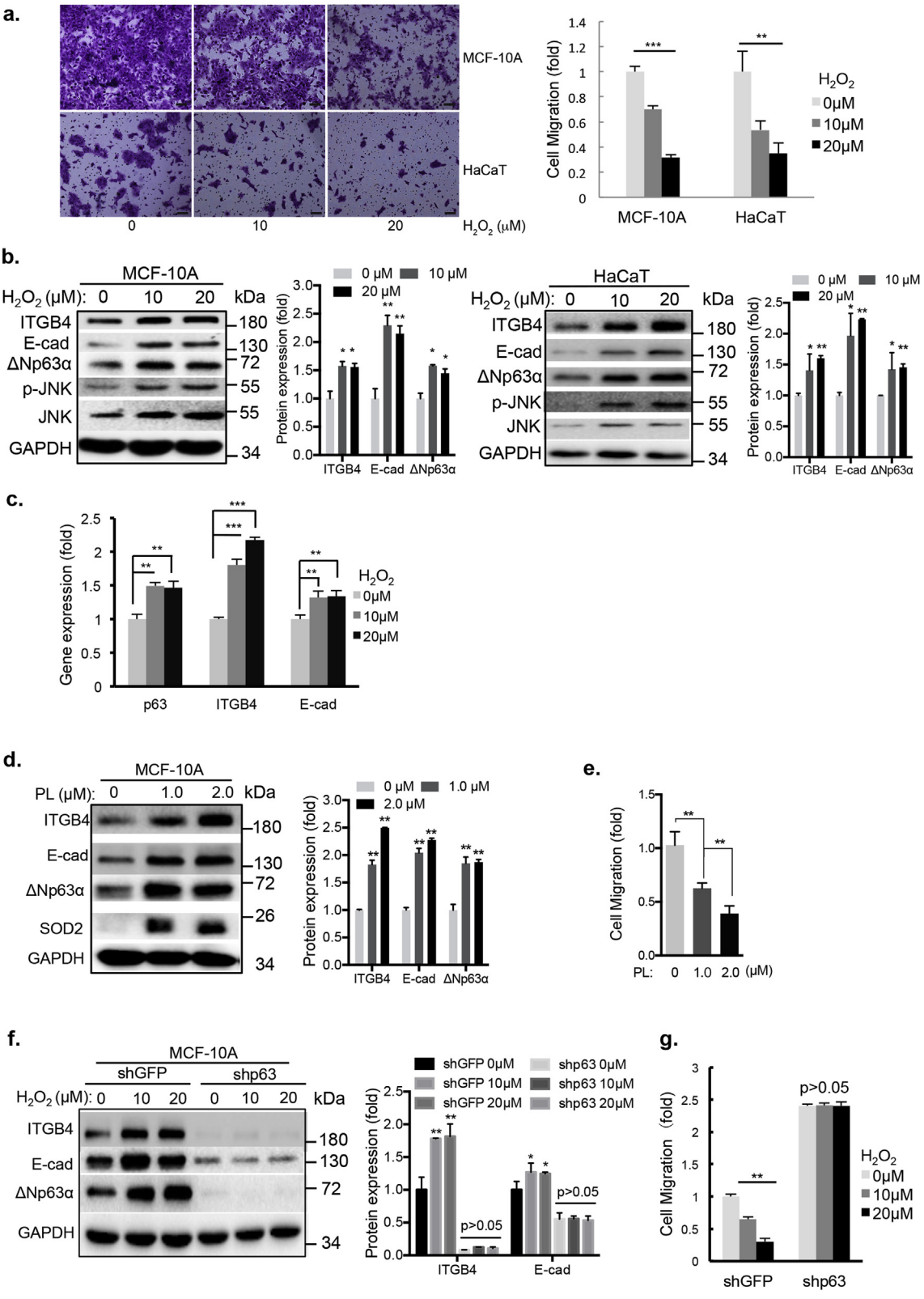

(caption on next page)

ΔNp63α expression is frequently observed in advanced human cancers.

In this study, we demonstrate that MST2 is critical in oxidative stress-induced inhibition of cell migration in vitro and tumor metastasis in vivo. Oxidative stress activated MST1/2, resulting in upregulation of ΔNp63α expression in a FoxO3a-dependent manner. In addition, ablation of MST1 or MST2 impacted the expression of a different subset of genes involved in cell-cell adhesion and cell mobility. Loss of MST1 led to robust reduction of E-cadherin and disruption of cell-cell adhesion leading to scattered cell growth in vitro, while loss of MST2 resulted in robust reduction of integrin β4, and consequently, increased cell mobility in vitro and tumor metastasis in vivo.

Fig. 1. Induction of ROS inhibits cell migration via upregulation of ΔNp63α expression. (a) MCF-10A or HaCaT cells were treated with an indicated dose of H_2O_2 for 24 h and then subjected to transwell assays for cell migration. Migrated cells were fixed and stained with crystal violet. Representative images were shown (left panels). Scale bar = 100 μm. The quantitative data from migration were presented as the means ± S.E. from three independent experiments in duplicate. ***p < 0.001; **p < 0.01. (b) MCF-10A or HaCaT cells were treated with H_2O_2 at indicated doses for 12 h. Cell lysates were subjected to Western blotting using a specific antibody as indicated. The data from quantitative analyses were shown as the means ± S.E. from two independent experiments. *p < 0.05; **p < 0.01. (c) MCF-10A cells were treated with an indicated dose of H_2O_2 for 12 h. Total RNA was extracted and subjected to Q-PCR analyses for steady-state mRNA levels of pan-p63, integrin β4 or E-cadherin. Data were presented as the means ± S.E. from three independent experiments in duplicate. ***p < 0.001; **p < 0.01. (d–e) MCF-10A cells were treated with piperlongumine (PL) for either 12 h prior to Western blot analyses and the quantitative data from two independent experiments were shown (d); or 24 h prior to transwell assays (e). The quantitative data from migration were presented as the means ± S.E. from three independent experiments in duplicate. **p < 0.01. (f–g) MCF-10A cells stably expressing shRNA specfic for pan-p63 or a control shRNA (shGFP) were treated with H_2O_2 at an indicated dose for either 12 h prior to Western blot analyses and the quantitative data from two independent experiments were shown (f); or 24 h prior to transwell assays (g). The quantitative data from migration assays were presented as the means ± S.E. from three independent experiments in duplicate. *p < 0.05; **p < 0.01. . (For interpretation of the references to colour in this figure legend, the reader is referred to the Web version of this article.)

2. Materials and methods

2.1. Cell culture and drug treatment

MCF-10A cells were cultured with 5% fetal bovine serum (HyClone, Utah, USA), supplemented with penicillin (100 U/ml)/streptomycin (100 μg/ml) (HyClone, Utah, USA), 20 ng/ml epidermal growth factor (Invitrogen), 100 ng/ml cholera toxin (Sigma), 10 mg/ml insulin (Sigma) and 500 ng/ml hydrocortisone (Sigma) in Dulbecco's modified Eagle's medium (DMEM)/F12 (Gibco, NY, USA). HaCaT and HEK-293T cells were cultured with 10% FBS supplemented with penicillin (100 U/ml)/streptomycin (100 μg/ml) in DMEM (Gibco, NY, USA). Cells were cultured at 37 °C in a humidified 5% CO_2 incubator.

Hydrogen peroxide (H_2O_2) was freshly diluted in PBS (pH7.4) and used at a designated final concentration. Piperlongumine (PL) (S7551, Selleck, Texas, USA) was dissolved in dimethyl sulfoxide (DMSO) at a stock concentration of 10 mM and used at designated final concentrations (0–2 μM).

2.2. Plasmids and lentiviral infection

Short hairpin RNAs (shRNA) specific for GFP, human p63, MST1 or MST2 were cloned into pLKO.1-puro vectors. Targeted sequences are listed in Supplemental Table S1. Recombinant lentiviruses including pLVX-ΔNp63α, pLVX-FoxO3a-GFP or pLVX-E-cadherin were amplified in HEK-293T cells as described [19].

2.3. Western blot analysis and immunofluorescence

Western blot analyses and immunofluorescence were performed as described [19]. Antibodies specific for p63 (sc-8431), YAP (sc-398182) or integrin β4 (sc-135950) were purchased from Santa Cruz Biotechnology (CA, USA); Antibody specific for FoxO3a (2497), MST1 (3682), MST2 (3952), phospho-MST1 (Thr183)/MST2(Thr180) (3681), JNK (9252), phospho-JNK (9251) or PI3 Kinase p110α (4249) were purchased from Cell Signaling Technology (MA, USA); Antibodies specific for E-cadherin (1702-1), AKT1 (1081-1), phospho-ATK(T308) (2214-1), or SOD2 (2299-1) were purchased from Epitomics (Burlingame, CA, USA). An antibody specific for HER2 (AH210) was purchased from Beyotime Biotechnology (Shanghai, China); and an antibody specific for GAPDH (340424) was purchased from Zen BioScience (Chengdu, China). Goat anti-mouse IgG-HRP (sc-2005) or goat anti-rabbit IgG-HRP (sc-2004) antibodies were purchased from Santa Cruz Biotechnology (CA, USA); Rhodamine (TRITC)–conjugated AffiniPure Donkey Anti-Rabbit IgG (711-025-152) used for immunostaining was from purchased from Jackson Immuno Research (PA, USA).

2.4. Cell migration assay

Cell migration assays were performed using transwell membrane filter inserts in 24- well tissue culture plates (BD Biosciences, USA). MCF-10A cells (5×10^4) or HaCaT cells (1×10^5) were suspended in serum-free medium and subjected to transwell assays as described [19].

2.5. Quantitative PCR (Q-PCR) analyses

Total RNA was isolated using an innuPREP RNA Mini Kit (Analytik Jena, Germany), followed by reverse transcription using ReverTra Ace qPCR RT Master Mix (TOYOBO, Osaka, Japan) according to the manufacturer's instructions. Q-PCR was performed in a Real-Time PCR System (Applied Biosystems, CA, USA) using a QuantiTect SYBR Green PCR Kit (Qiagen, Hilden, Germany) according to the manufacturer's instructions. Sequences of specific primers used for Q-PCR are listed in Supplemental Table S2.

2.6. Cell cycle and viability analyses

Cell cycle analyses were performed by fluorescence activated cell sorting (FACS). Cells were collected and fixed in 70% ethanol at 4 °C overnight and stained with 50 μg/ml propidium iodide (PI, Sigma) supplemented with 100 μg/ml RNase A (Sigma) for 40 min at 37 °C in the dark. Cells were then analyzed by a FACScan flow cytometer (Becton Dickson, CA, USA). Cell viability was determined by MTS assay [19]. Then, 5000 cells/well were seeded in 96-well plates. After 12 h of incubation, cells were treated with or without designated chemicals for the indicated times and subjected to MTS assays as described.

2.7. Tumor metastasis in mice

Six-week old female nude mice were used for tumor metastasis assays. MCF-10A cells stably expressing HER2 were infected by lentivirus expressing ΔNp63α or shRNA against MST2 and puromycin-resistant cells were selected. Then, 1.5×10^6 cells derived from four different groups (control, HER2, HER2/shMST2, or HER2/shMST2/ΔNp63a) in 0.15 ml physiological saline were injected into the tail vein of mice with eight mice per group. After 60 days, the mice were euthanized and the lungs were dissected and examined for metastatic nodules. The lungs were fixed in 3.7% formaldehyde, embedded in paraffin, and sliced for hematoxylin and eosin (H&E) staining and histological analysis.

2.8. MMTV-PyMT tumor model

FVB/N-Tg (MMTV-PyMT) 634Mul-transgenic female virgin mice were grown for 95 days before being sacrificed. Then, whole mammary glands, tumors and lungs were removed. Formalin fixed, paraffin embedded mammary glands, tumors, and lungs were sectioned at 5 μm. All animal experiments in this study were approved by the Institutional Animal Care and Use Committee (IACUC) of Sichuan University, and the procedures were performed according to the guidelines established by the China Council on Animal Care.

2.9. ROS measurement

ROS levels in MCF-10A cells were determined using a Reactive

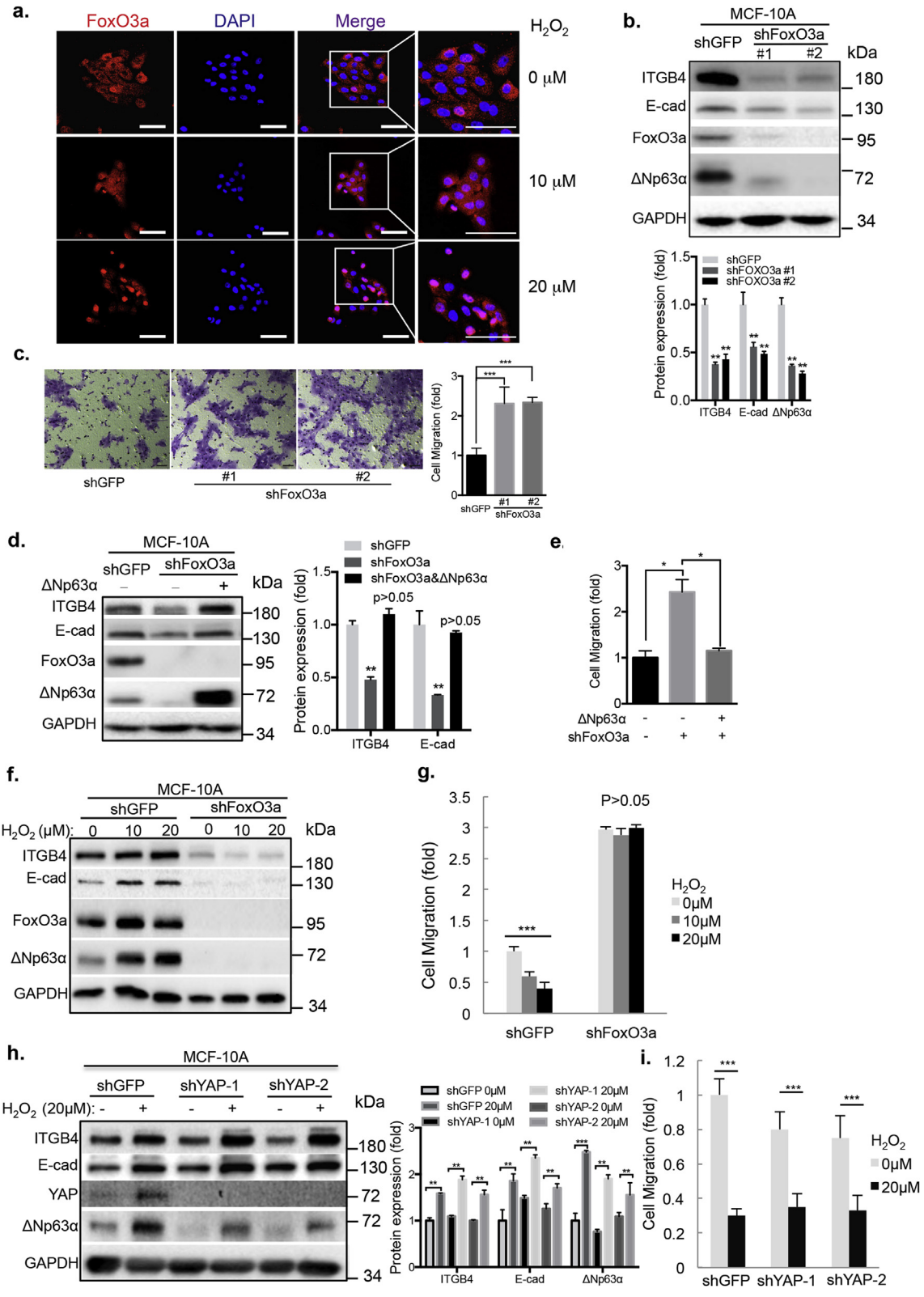

(caption on next page)

Oxygen Species Assay Kit (Beyotime, Shanghai, China) according to the manufacturer's instructions. Briefly, after treatment with H_2O_2 or PL, MCF-10A cells were incubated with DCFH-DA at 37 °C and were then subjected to FACS to measure fluorescence intensity.

2.10. Immunohistochemistry (IHC) analyses of tumor tissues and average optical density (AOD) measurement

Mammary tumor samples derived from MMTV-PyMT mice were subjected to IHC using specific antibodies as indicated. Human tissue arrays containing consecutive sectioning of human breast cancer

Fig. 2. H_2O_2 promotes FoxO3a nuclear localization and ablation of FoxO3a facilitates cell migration via downregulation of ΔNp63α in a YAP-independent manner. (a) MCF-10A cells were treated with H_2O_2 at an indicated dose for 12 h and were then subjected to immunostaining using an antibody specific for FoxO3a (red). Nuclei were counterstained with DAPI (blue). Scale bar = 50 μm. (b–c) MCF-10A cells stably expressing shRNA specific for FoxO3a (#1 or #2) or a control shRNA (shGFP) were subjected to Western blot analyses and the quantitative data from two independent experiments were shown (b) or to transwell assays (c). Representative images were shown (Left panels). Scale bar = 100 μm. The quantitative data from migration assays were presented as means ± S.E. from three independent experiments in duplicate. **p < 0.01; ***p < 0.001. (d–e) MCF-10A cells expressing shGFP or shFoxO3a (#2) were infected with lentivirus expressing ΔNp63α or a vector control. Stable cells were subjected to Western blot analyses and the quantitative data from two independent experiments were shown (d) or transwell assays (e). The quantitative data from migration assays were presented as the means ± S.E. from three independent experiments in duplicate. *p < 0.05; **p < 0.01. (f–g) MCF-10A cells stably expressing shFoxO3a or shGFP were treated with H_2O_2 at an indicated dose and were then subjected to Western blot (f) or transwell assays (g). The quantitative data from migration assays were presented as the means ± S.E. from three independent experiments in duplicates. ***p < 0.001. (h–i) MCF-10A cells stably expressing shYAP (shYAP-1 and shYAP-2) or shGFP in the presence or absence of H_2O_2 were subjected to Western blot and the quantitative data from two independent experiments were shown (h) or transwell assays (i). The quantitative data from migration assays were presented as the means ± S.E. from three independent experiments in duplicate. **p < 0.01; ***p < 0.001. . (For interpretation of the references to colour in this figure legend, the reader is referred to the Web version of this article.)

carcinoma biopsy samples and paired tumor-adjacent tissue sections were obtained from OUTDO (Shanghai, China). Tissue array slides were subjected to IHC using a specific antibody as indicated and slides were then scanned through NanoZoomer (Hamamatsu, Japan). Scanned images were then subjected to integrated optical density (IOD) measurements via Image-Pro Plus 6.0 to calculate average optical density (AOD) using the formula: AOD = IOD/Area [20].

2.11. Statistical analysis

Student's t-test was used for analyses that involved only two groups for comparison, and ANOVA tests were used for analyses that involved more than two groups for comparisons. Data are presented as the means ± standard error (S.E.). Pearson's correlation was conducted with SPSS version 20.0 software (IBM/SPSS, Chicago, IL, USA).

3. Results

3.1. Oxidative stress upregulates ΔNp63α expression and inhibits cell migration

Reactive oxygen species (ROS) plays a critical role in the regulation of various biological processes, including cell cycle, apoptosis, cellular senescence, autophagy, and metabolism. However, the precise role for ROS in cell mobility remains elusive. To investigate the effect of moderate ROS on cell migration, we treated untransformed human breast epithelial MCF-10A, human immortalized keratinocyte HaCaT, human squamous cell carcinoma FaDu and human triple negative breast cancer HCC1806 cells with a moderate dose of H_2O_2 (10 or 20 μM). As shown in Fig. 1a and Supplemental Fig. S1a, treatment of H_2O_2 led to a dose-dependent inhibition of cell migration in those cells. At the molecular level, H_2O_2 induced the phosphorylation of JNK, as expected, consistent with previous studies [21]. Notably, the expression of ΔNp63α, a critical regulator of cell adhesion and mobility [18], was markedly upregulated, concomitant with increased expression of ITGB4 and E-cadherin (Fig. 1b), both of which are downstream targets of ΔNp63α [18].

Next, we investigated the molecular basis on which oxidative stress induces the expression of ΔNp63α, ITGB4 and E-cadherin. As shown in Fig. 1c, quantitative PCR (Q-PCR) analyses showed that H_2O_2 significantly upregulated steady-state mRNA levels of ΔNp63α, ITGB4 or E-cadherin, suggesting a transcriptional upregulation of these genes in response to oxidative stress. To verify that ROS can indeed impact the expression of ΔNp63α, ITGB4 and E-cadherin, we used piperlongumine (PL), a strong ROS inducer [22], in our experimental system. As shown in Fig. 1d, while treatment of PL activated SOD2, as expected [23], PL significantly upregulated expression of ΔNp63α, ITGB4 and E-cadherin. Importantly, PL significantly inhibited cell migration in a dose-dependent manner (Fig. 1e). Upon measurement of ROS levels, it was evident that H_2O_2 or PL significantly upregulated cellular ROS levels (Supplemental Figs. S1b–1c).

We then examined whether H_2O_2 impacts the migration of Her2/PI3K activated cells. As shown in Supplemental Figs. S1d–1e, HER2 expression significantly suppressed ΔNp63α protein levels, consistent with our previous study [19]. Notably, HER2 also significantly inhibited expression of integrin β4 and E-cadherin. Treatment with H_2O_2 markedly reversed the expression of ΔNp63α and integrin β4 while it had much less of an effect on E-cadherin expression. Consequently, H_2O_2 significantly reversed HER2-induced cell migration. Similar phenomena were observed in PL-treated cells with expression of activated $p110\alpha^{H1047R}$, a hotspot mutation on the PIK3CA gene [24] (Supplement Figs. S1f–1g). These data demonstrate that elevated ROS leads to upregulation of ΔNp63α resulting in suppression of oncogene-induced cell migration.

We next investigated whether ΔNp63α plays a causative role in oxidative stress-mediated inhibition of cell migration. We used a shRNA for pan-specific p63, which effectively silenced expression of ΔNp63α [19]. As shown in Fig. 1f, silencing of ΔNp63α completely blocked the H_2O_2-induced upregulation of ITGB4. By contrast, the expression of E-cadherin was significantly reduced, but not completely vanished under similar conditions, suggesting that ΔNp63α differently impacts the expression of ITGB4 and E-cadherin in response to oxidative stress. Notably, H_2O_2 was unable to inhibit cell migration upon ΔNp63α ablation (Fig. 1g), demonstrating that ΔNp63α expression is essential for oxidative stress-induced inhibition of cell migration.

As ROS can have cytotoxic effects, promoting cell cycle arrest and cell death [25], we therefore examined the effects of an oxidative stress inducer on either the cell cycle or cell viability. Under our experimental setting, neither cell cycle nor cell viability was significantly altered in MCF-10A cells (Supplemental Figs. S2a–2b). Taken together, these data indicate that oxidative stress upregulates the expression of ΔNp63α, ITGB4 and E-cadherin, which in turn inhibits cell migration in a ΔNp63α-dependent manner.

3.2. Oxidative stress induces FoxO3a nuclear accumulation and ΔNp63α expression, resulting in inhibition of cell migration independent of YAP

The aforementioned data indicates that oxidative stress upregulates the expression of ΔNp63α, resulting in inhibition of cell migration. Because ΔNp63α is a direct transcriptional target of FoxO3a [19], we therefore investigated whether FoxO3a plays a role in oxidative stress-mediated upregulation of ΔNp63α. With this regard, we first examined the subcellular localization of FoxO3a in the presence or absence of H_2O_2. As shown in Fig. 2a, H_2O_2 significantly induced nuclear accumulation of FoxO3a in a dose-dependent manner. Knockdown of FoxO3a dramatically reduced the expression of ΔNp63α, ITGB4 or E-cadherin in MCF-10A cells (Fig. 2b). Ablation of FoxO3a also resulted in significantly reduced expression of ΔNp63α, ITGB4 and E-cadherin in HaCaT cells (Supplemental Fig. S3a). Furthermore, knockdown of FoxO3a significantly accelerated cell migration, which was remarkably rescued by ectopic expression of ΔNp63α (Fig. 2c-e and Supplemental Fig. S3b). Moreover, knockdown of FoxO3a completely eliminated

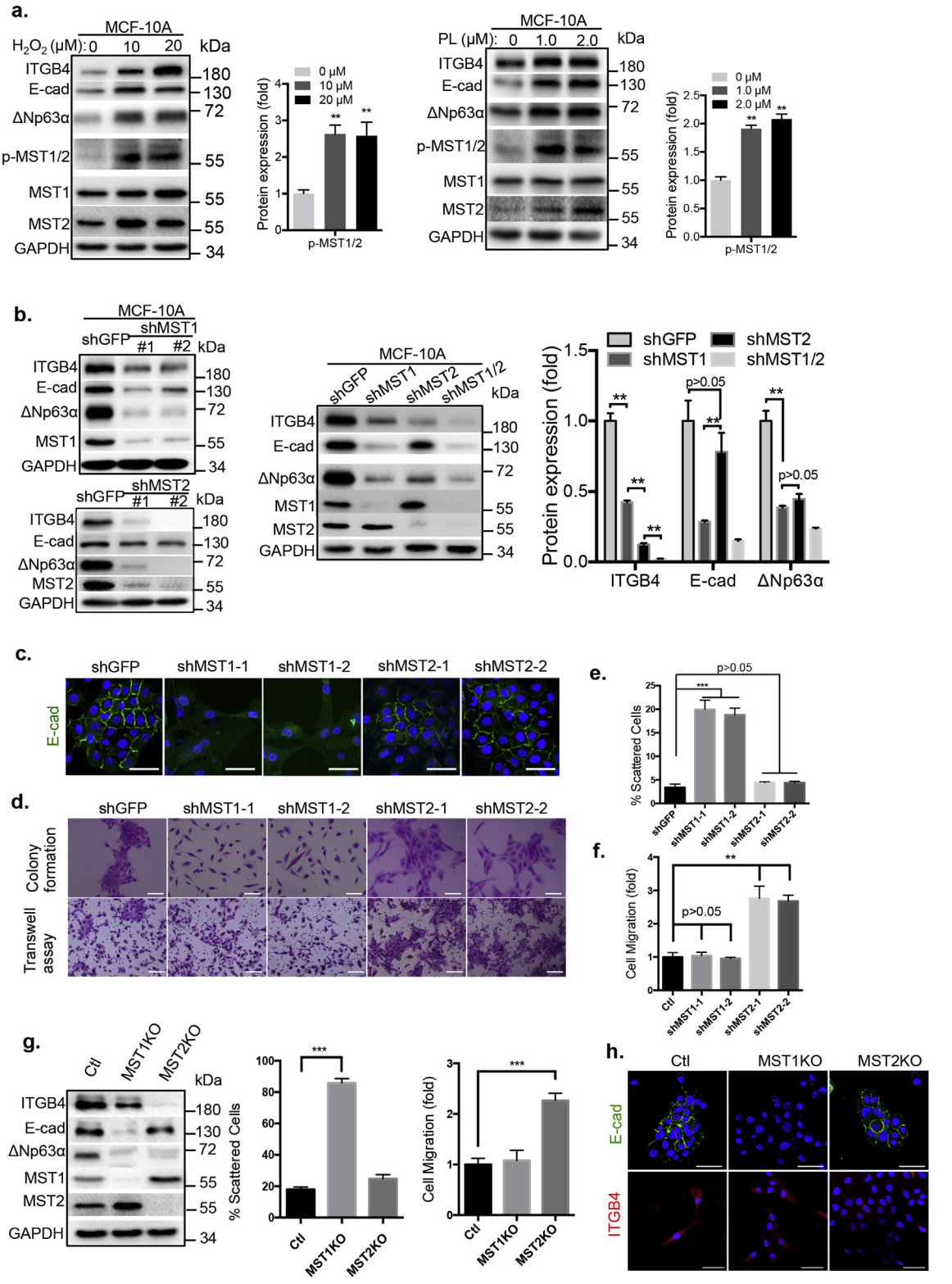

(caption on next page)

H_2O_2-induced upregulation of ΔNp63α, ITGB4 and E-cadherin, resulting in a complete reversal of H_2O_2-induced cell migration inhibition (Fig. 2f-g). Together, these data suggest that FoxO3a is most likely responsible for H_2O_2-mediated regulation of cell mobility.

YAP has been reported as an important player mediating ROS signaling [26]. We therefore examined the role for YAP in H_2O_2-mediated inhibition of cell migration. As shown in Fig. 2h-i, H_2O_2 upregulated YAP expression, concomitant with elevated ΔNp63α protein levels. Knockdown of YAP led to a significantly reduced ΔNp63α expression, consistent with previous reports that YAP positively regulates ΔNp63α [27,28]. However, in response to H_2O_2, ΔNp63α, as well as ITGB4 and E-cadherin, was still significantly elevated although expressed less in the absence of detectable YAP protein, suggesting that H_2O_2 upregulates ΔNp63α primarily in a YAP-independent manner. Importantly,

Fig. 3. H_2O_2 induces the phosphorylation of MST1/2 and ablation of MST1 leads to the suppression of E-cadherin expression and scattered cell growth whereas ablation of MST2 inhibits integrin β4 expression and facilitates cell migration. (a) MCF-10A cells were treated with an indicated dose of H_2O_2 or PL for 12 h. Cell lysates were subjected to Western blotting using a specific antibody as indicated and the quantitative data from two independent experiments were shown. $^{**}p < 0.01$. (b–f) Stable MCF-10A cells expressing one of two different shRNAs specific for MST1 (shMST1-#1; shMST1-#2), MST2 (shMST2-#1; shMST2-#2) or a control shRNA (shGFP) were subjected to Western blotting using a specific antibody as indicated and the quantitative data from two independent experiments were shown (b). Stable cells were subjected to IHC for E-cadherin. Representative micrographs were shown. Scale bar = 50 μm (c). Cells were seeded in 6-well plates for 20 h, and cells were then fixed and stained using crystal violet (d, upper panel). Percentage of scattered cells was defined as the ratio of scattered cells (≤3 cells per colony) to total cells counted from three independent experiments in duplicate. Scale bar = 100 μm (e); In parallel, cells were subjected to transwell assays for cell migration (d, lower panel). Scale bar = 100 μm. The quantitative data from migration assays were quantified and presented as the means ± S.E. from three independent experiments in duplicate (f); $^{**}p < 0.01$; $^{***}p < 0.001$. (g) Single clones of MCF-10A cells with either MST1 or MST2 knockout were obtained by the Crispr-Cas9 system. MCF-10A-MST1KO or MCF-10A-MST2KO cells were subjected to Western blotting (left panel), a cell-scattering assay (middle panel) and transwell assays (right panel). Data were quantified and presented as the means ± S.E. from three independent experiments in duplicates. $^{***}p < 0.001$. (h) MCF-10A-MST1KO or MCF-10A-MST2KO cells were subjected to immunostaining using an antibody specific for E-cadherin (upper panel) or ITGB4 (lower panel). Nuclei were counterstained with DAPI. Scale bar = 50 μm. . (For interpretation of the references to colour in this figure legend, the reader is referred to the Web version of this article.)

knockdown of YAP had little effect on H_2O_2-mediated inhibition of cell migration.

3.3. MST1 and MST2 have distinct functions in the regulation of cell adhesion programs and cell migration

Our aforementioned data indicates that H_2O_2 upregulates ΔNp63α expression, resulting in inhibition of cell mobility largely independent of YAP. It has been reported that H_2O_2 can induce the phosphorylation of MST1 on the T183 residue and MST2 on T180 residue. Activated MST1 in turn facilitates phosphorylation at S207 of FoxO3a, leading to its nuclear accumulation thereby triggering an apoptotic response independent of YAP [12]. Therefore, we investigated whether MST1/MST2 are involved in oxidative stress-mediated regulation of cell mobility. Under our experimental setting, treatment with either H_2O_2 or PL clearly induced the phosphorylation of MST1 and MST2, concomitant with increased expression of ΔNp63α, ITGB4 and E-cadherin in MCF-10A cells (Fig. 3a) and in HCC1806 or FaDu cells (Supplemental Fig. S3c). We then investigated the role for MST1 or MST2 in oxidative stress-induced alteration of cell mobility. As shown in Fig. 3b, knockdown of either MST1 or MST2 led to a significant down regulation of ΔNp63α. By sharp contrast, ablation of MST1 dramatically reduced the expression of E-cadherin whereas ablation of MST2 led to a dramatic reduction of ITGB4 expression. Simultaneous knockdown of MST1 and MST2 completely eliminated the expression of ITGB4, while the expression of E-cadherin was comparable to that of MST1 knockdown (Fig. 3b, right panel). Notably, knockdown of ITGB4 led to a significant increase in cell migration (Supplemental Figs. S3d–3e).

Oue aforementioned data indicated that H_2O_2 upregulated ΔNp63α levels in the absence of YAP expression suggesting a YAP-independent manner. We furthermore examined the effects of H_2O_2 on YAP cellular sublocalization. As shown in the Supplemental Fig. S4a, treatment with a moderate dose of H_2O_2 (20 μM) at 1 or 12 h used in our experimental settings did not promote YAP nuclear translocation, while high dose of H_2O_2 (400 μM) treated for 1 h significantly induced YAP nuclear localization, as reported [29]. Notably, Knockdown of either MST1 or MST2 was unable to promote YAP nuclear localization in response to H_2O_2 (20 μM) at 1 or 12 h, suggesting, again, MST1/2 regulates ΔNp63α independent of YAP in response to a moderate dose level of H_2O_2.

Importantly, ablation of MST1 resulted in vanished expression of E-cadherin as evidenced by immunofluorescence staining (Fig. 3c) accompanied with scattered cell growth [30] (Fig. 3d-upper panel and 3e). By contrast, although ablation of MST2 led to reduced expression of E-cadherin, it did not result in scattered cell growth. Strikingly, while ablation of MST2 significantly facilitated cell migration, ablation of MST1 had little effect on cell mobility (Fig. 3d and f). Thus, these data indicate that MST2 is critical in the modulation of cell mobility whereas MST1 is important in cell-cell adhesion in vitro (Fig. 3f).

To further confirm that MST1 and MST2 possess distinct biological functions in the regulation of cell mobility, we established MST1 knockout (MST1KO) or MST2 knockout (MST2KO) cell lines using the CRISPR-Cas9 system. As shown in Fig. 3g, MST1KO or MST2KO cells exhibited distinct regulation on E-cadherin and ITGB4, reflecting exactly the same changes observed in shMST1/shMST2 cells. Again, cell migration and scattered cell growth in vitro were affected by MST2KO or MST1KO, respectively (Fig. 3g, middle and right panels, respectively). In addition, while the expression of E-cadherin was evident in MST2KO cells, it was barely detectable in MST1KO cells (Fig. 3h, upper panel). By contrast, the expression of ITGB4 was readily detectable in MST1KO cells but it was vanished in MST2KO cells (Fig. 3h, lower panel).

3.4. MST2 activates the FoxO3a-ΔNp63α-ITGB4 axis to inhibit cell migration in response to oxidative stress

Because MST1 phosphorylates FoxO3 proteins and promotes FoxO3 nuclear translocation to induce cell death upon treatment of 100 μM H_2O_2[13], we examined whether MST2 also plays a role in FoxO3 nuclear translocation. As shown in Fig. 4a, treatment of 20 μM H_2O_2 effectively induced nuclear accumulation of FoxO3a-GFP stably expressed in MCF-10A cells [12], which was significantly blocked by ablation of either MST1 or MST2. Since ablation of MST2, but not MST1, induces cell migration, we therefore examined whether ectopic expression of FoxO3a can reverse MST2 ablation-induced cell migration. As shown in Fig. 4b-c, again, ablation of MST2 led to a significantly reduced expression of ΔNp63α at both mRNA and protein levels, which was effectively restored by FoxO3a expression. Importantly, the expression of FoxO3a markedly reversed MST2-ablation-induced cell migration (Fig. 4d). In addition, the expression of ΔNp63α effectively blocked cell migration promoted by MST2 ablation (Fig. 4e-f). Together, these data suggest that MST2 regulates cell migration via modulation of the FoxO3a-ΔNp63α axis.

We next investigated the role for MST2 in oxidative stress-mediated inhibition of cell migration. As shown in Fig. 4g, ablation of MST2 not only robustly inhibited the expression of ΔNp63α and ITGB4, but it also completely blocked H_2O_2-induced upregulation of these proteins. Importantly, oxidative stress-mediated inhibition of cell migration was completely eliminated in the absence of MST2 in MCF-10A cells (Fig. 4g and h) or in HaCat, HCC1806, or FaDu cells (Supplemental Fig. S4b). In addition, Knockdown of ITGB4 almost completely reversed H_2O_2-mediated inhibition of cell migration in MCF-10A cells (Fig. 4i and j).

Because the ablation of MST1 dramatically downregulates ΔNp63α and E-cadherin expression, concomitant with scattered cell growth (Fig. 3c-3e), we reasoned that reduced ΔNp63α/E-cadherin may be responsible for the observed scattered cell growth. We therefore performed rescuing experiments. Restoration of E-cadherin expression led to effective cell-cell adhesion as evidenced by the typical appearance of colony formation whereas restoration of ΔNp63α expression largely but not completely restored the expression of E-cadherin, concomitant with partially rescued scattered cell growth (Supplemental Figs. S4c–S4d).

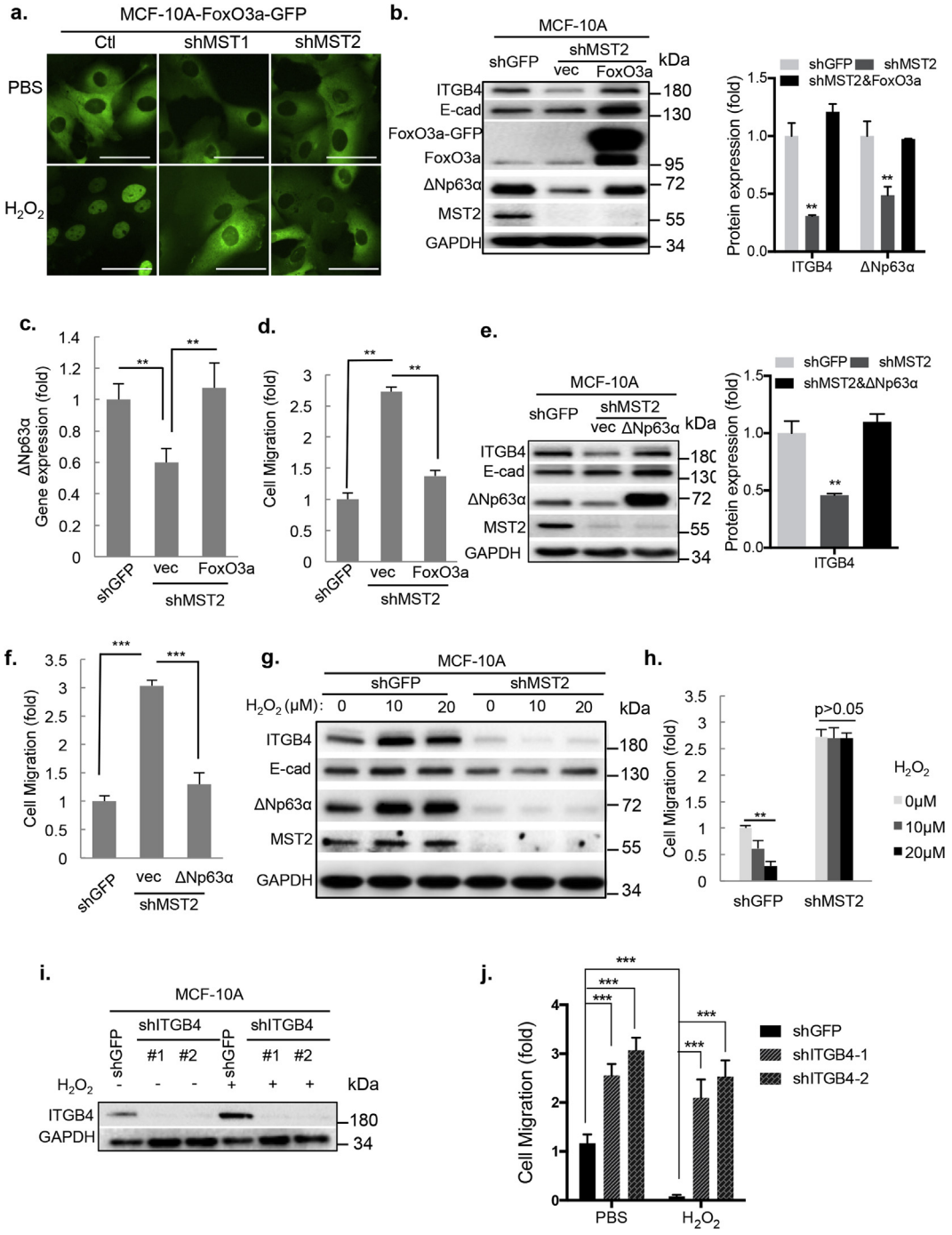

Fig. 4. Ablation of MST2 inhibits H_2O_2-induced FoxO3a nuclear localization, resulting in suppression of ΔNp63α expression and increased cell migration. (a) MCF-10A cells stably expressing FoxO3a-GFP were treated with 20 μM H_2O_2 for 2 h and were then directly subjected to fluorescence microscopy to capture fluorescence images. Scale bars = 50 μm. (b–f) In rescuing experiments, stable MCF-10A-shMST2-1 or MCF-10A-shGFP cells were infected with lentivirus expressing either FoxO3a or ΔNp63α and a vector control (vec). Puromycin-resistant cells were subjected to Western blotting and the quantitative data from two independent experiments were shown (b and e). Q-PCR analyses for pan-p63 expression (c) or transwell assays for cell migration for 24 h (d and f), data were quantified and presented as the means ± S.E. from three independent experiments in duplicate. **$p < 0.01$; ***$p < 0.001$. (g–h) Stable MCF-10A-shMST2-1 or MCF-10A-shGFP cells were treated with an indicated dose of H_2O_2 for 12 h. Cells were then subjected to Western blotting (g) or transwell assays for 24 h (h). The quantitative data from migration assays were quantified and presented as the means ± S.E. from three independent experiments in duplicate. **$p < 0.01$. (i–j) Stable MCF-10A cells expressing shITGB4 (#1 or #2) were treated with an indicated dose of H_2O_2 for 12 h. Cells were then subjected to Western blotting (i) or transwell assays for 24 h (j). The quantitative data from migration assays were quantified and presented as the means ± S.E. from three independent experiments in duplicate. ***$p < 0.001$.

These data suggest that ΔNp63α is critically important, but not the only factor, in the regulation of E-cadherin.

Reduced expression of p-MST1/2 and p63 in the MMTV-PyMT mouse mammary tumor and clinical breast cancer samples.

To investigate clinical relevance, we examined the expression of MST1, MST2, p-MST1/2, p63 and ITGB4 in human breast carcinoma biopsy samples and paired adjacent tissue via IHC (Fig. 5a) followed by measured Average Optical Density (AOD) analyses [20] (Fig. 5c), which showed significant downregulation of MST1, MST2, p-MST1/2, p63 and ITGB4 expression in breast carcinoma compared to the paired adjacent

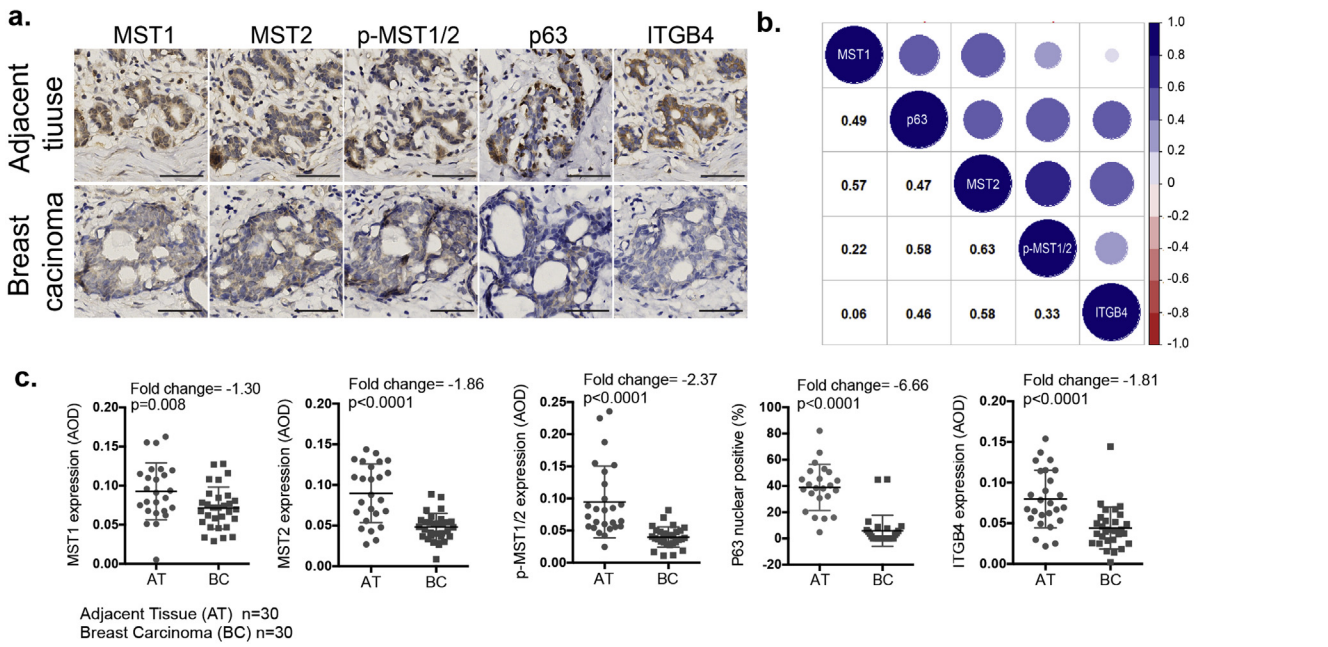

(caption on next page)

Fig. 5. Expression of pMST1/2 and p63 is reduced in the MMTV-PyMT mouse mammary tumor and clinical breast cancer samples. Also, ablation of MST2 facilitates lung metastasis reversed by restoration of ΔNp63α expression. (a–c) Consecutive sections of human breast carcinoma biopsy samples and adjacent normal tissue were subjected to IHC staining (Scale bars = 100 μm) (a), and to quantitative analyses for correlation between MST1, MST2, p-MST1/2, p63 or ITGB4 (b–c). (d) Hyperplasia mammary tissues, primary mammary primary tumors and lung metastasis nodules derived from the same MMTV-PyMT mouse (n = 5) were subjected to IHC using a specific antibody as indicated. Representative IHC images from two MMTV-PyMT mice (#1 and #2) were shown. Scale bar = 100 μm. (e–i) MCF-10A cells stably expressing vectors, HER2, HER2-shMST2, or HER2-shMST2-ΔNp63α were subjected to Western blotting (e), transwell assays (f) or were used to intravenously inject nude mice (1.5×10^6 cells). The mice were observed daily and euthanized after 45 days. (g) Lungs were dissected, fixed and inspected for metastatic nodules on their surface. Arrows point to metastatic nodules. (h) Graph represents the number of metastatic nodules in the lungs per mouse. A horizontal line indicates the mean for each group. (i) Lungs were fixed, embedded in paraffin, sectioned, and stained by hematoxylin and eosin (H&E) for histological analysis. Scale bar = 200 μm *p < 0.05; **p < 0.01; ***p < 0.001.

tissues. Notably, in keeping with aforementioned data, there was a significantly positive correlation between p63 and MST1/MST2. Most interestingly, there was a strong correlation between ITGB4 and MST2, but not with MST1.

We further investigate the correlation between MST1/2 expression and tumor development in mammary tissues of hyperplasia, primary mammary tumors, and lung metastasis nodules derived from MMTV-PyMT FBV mice, a frequently used genetic mammary tumor mouse model [31]. As shown in Fig. 5d, the expression of MST2, p-MST1/2, p63 and ITGB4 was readily detectable in hyperplasia tissue samples but was significantly reduced in primary tumors or in lung metastasis nodules. These data suggest that the expression of MST1 and MST2 is differentially regulated and that the reduced expression of MST2 and/or phosphorylated MST1/MST2 closely correlates with mammary tumor development.

3.5. Ablation of MST2 facilitates tumor metastasis reversed by the restoration of ΔNp63α

Next, we examined the effects of MST2 ablation on the metastasis potential of MCF-10A-Her2 cells using a tail-vein injection mouse model [32]. Stable expression of Her2 in MCF-10A cells (MCF-10A-Her2) promotes metastasis in this model [19,32]. As shown in Fig. 5e and f, Her2 expression in MCF-10A cells markedly downregulated ΔNp63α expression, consistent with our previous work [32]. ΔNp63α expression was completely inhibited by additional MST2 knockdown, resulting in a significant increase in cell mobility, which was effectively reversed by restoration of ΔNp63α expression. These cells were then used to evaluate tumor metastatic potential in mice. As shown in Fig. 5g and h, Her2-mediated tumor metastasis was further promoted by knockdown of MST2. Restoration of ΔNp63α expression effectively inhibited tumor metastasis in vivo. Furthermore, histological examination revealed normal lung architecture in control mice, while metastatic nodules were frequently observed in lungs derived from mice injected with MCF-10A-Her2/shMST2 cells. Restoration of ΔNp63α expression led to lungs with normal architectures (Fig. 5i).

3.6. Ablation of MST2 impacts the expression of a subset of genes involved in cell mobility

Our aforementioned data indicates that MST1 impacts cell-cell junction via modulation of E-cadherin expression whereas MST2 regulates cell mobility via ITGB4. To dissect the molecular basis that accounts for the related but distinct functions of MST2 and MST1, we examined transcriptomes of MCF-10A MST1KO or MST2KO cells. RNA-seq analyses of samples (normal, MST1KO and MST2KO) in triplicate were performed. Among approximately 28,000 transcripts analyzed, the expression of 325 genes and 469 genes were significantly upregulated (log2-fold change ≥ 3, P < 0.05) in MST1KO or MST2KO compared to normal control, respectively. While there were 82 overlapping genes, 243 and 387 genes were uniquely upregulated in MST1KO cells or MST2KO cells, respectively. In addition, the expression of 337 genes and 481 genes was significantly downregulated (log2-fold change ≤ −3, P < 0.05) in MST1KO or MST2KO compared to normal control, respectively, among which, there were 147 overlapping genes (Fig. 6a).

Further analyses revealed that MST1KO and MST2KO significantly impacted a different subset of genes involved in cell-cell junction, cell-matrix adhesion, cell-skeleton organization and EMT programs. As shown in the heatmap (Fig. 6b and Table 1), the expression of TP63 was significantly downregulated in both MST1KO and MST2KO, compared to controls. Notably, MST1KO primarily downregulates genes involved in cell junction including cell adherent junction, tight junction and desmosome. Specifically, the gene encoding E-cadherin (CDH1) critical for adherent junction and tight junction was dramatically downregulated. Other genes involved in tight junctions, including occludin (OCLN), claudin1 (CLDN1) and JAM-1 (F11R), were also significantly downregulated. Similarly, genes encoding desmoplakin (DSP) and plakoglobins (JUP), two most important components in desmosome, were dramatically decreased in MST1KO cells.

On the other hand, MST2KO also led to down regulation of genes involved in cell-cell junctions to a lesser extent (Fig. 6b and Table 1). Notably, unlike other tight junction-related genes, MPZL2 encoding myolin protein zero-like protein 2 [33] was significantly increased in MST2KO cells. Most strikingly, while MST1KO led to subtle differences, MST2KO resulted in dramatic upregulation of genes that facilitate cell migration, including genes involved cell-matrix adhesion (ITGA4, ITGB7, COL4A1, COL4A4, COL6A2, COL9A3) and cell skeleton organization (ACTRT3, FLNC, MYLK2). Furthermore, knockout of MST2 led to significant upregulation of genes that facilitate EMT, including SNAI1, RAC and PARVB. By contrast, wile MST1KO increased Slug (SNAI2) expression.

Importantly, The expression of ITGB4 was markedly downregulated in both MST1KO and MST2KO cells (0.67 vs. 0.62-fold changes compared to controls). Consistent with results from RNA-seq, Q-PCR analyses also showed that knockdown of either MST1 or MST2 led to significant downregulation of TP63, ITGB4 or E-cadherin (Supplemental Fig. S5a). However, the biochemical analyses indicated that MST2KO profoundly impacted ITGB4 expression much more significantly than that of MST1KO, raising the possibility that MST2 may affect ITGB4 expression in other ways. We therefore examined the effects of MST2KO on ITGB4 protein stability. Our data showed that knockout of MST2, but not MST1, significantly reduced ITGB4 protein levels, which was markedly reversed by treatment with proteasome inhibitor MG132 (Supplemental Fig. S5b). These results indicate that MST2 not only regulates ITGB4 gene transcription but also ITGB4 protein stability.

4. Discussion

ΔNp63α has been shown to inhibit oxidative stress-induced cell death and promote surivival [15,16]. In this study, we provide evidence that oxidative stress activates MST1/2 resulting in the upregulation of ΔNp63α and, consequently, the suppression of cell migration. Most interestingly, MST1 and MST2 significantly impact a different subset of genes involved in cell-cell junction or cell-matrix adhesion. In particular, the ablation of MST1 leads to the suppression of genes involved in cell-cell junction, resulting in scattered cell growth with little effect on cell migration. Ablation of MST2, on the other hand, leads to disruption of the cell-matrix adhesion, resulting in accelerated cell migration in vitro and facilitating tumor metastasis in vivo. In addition,

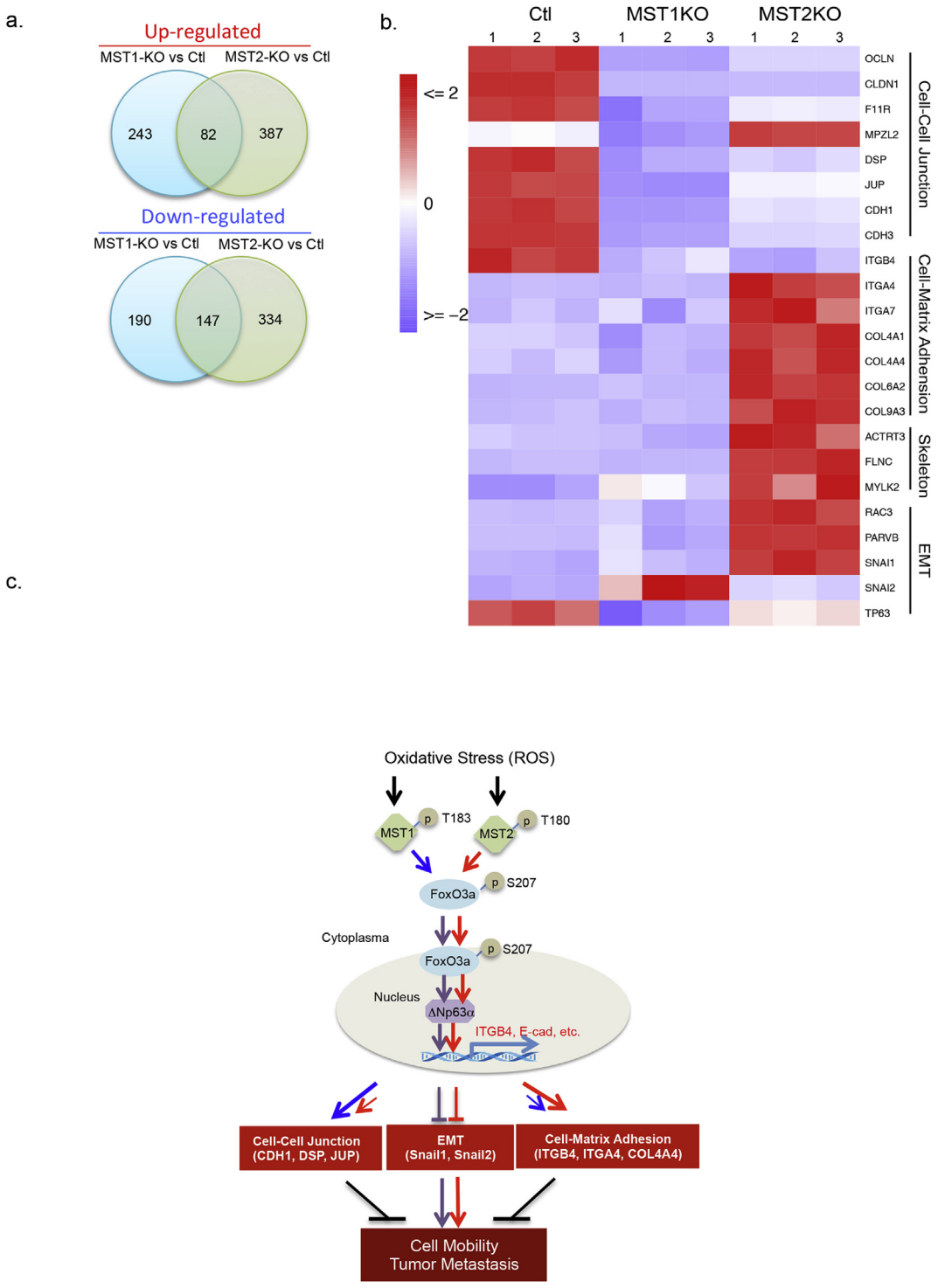

Fig. 6. The distinct functions of MST2 and MST1 in the regulation of cell junction and cell mobility. (a–b) MCF-10A, MCF-10A-MST1KO or MCF-10A-MST2KO cells were subjected to RNA-Seq analyses in triplicate. (a) Venn analysis, differentially expressed genes (log2-fold change ≥ 3, fold $P < 0.05$); (b) A heatmap showing changes of differentially expressed genes related to EMT, cell-cell junction, cell-matrix adhesion and skeleton organization; (c) A model of the Hippo kinase in the regulation of tumor metastasis upon oxidative stress. Oxidative stress activates MST1/2 by phosphorylation, which leads to the phosphorylation and nuclear accumulation of FoxO3a, resulting in upregulation of ΔNp63α. ΔNp63α in turn transactivates genes involved in EMT, cell-cell junction and cell-matrix adhesion. MST1 signaling is represented by blue arrows and blue lines, whereas MST2 signaling is represented by red arrows and red lines. . (For interpretation of the references to colour in this figure legend, the reader is referred to the Web version of this article.)

the expression of MST2 is significantly reduced in mammary tumors derived from the MMTV-PyMT mouse model and in human breast cancer samples. Consistent with our notion, several studies have shown that a reduced ΔNp63α expression in SCC, keratinocyte, or breast cancer cells leads to up-regulation of genes involved in cell motility and consequently promotes cell migration and invasion, while enforced ΔNp63α expression inhibits these traits [19,34,35]. Notably, it has been reported that transglutaminase 2 stimulates YAP-dependent ΔNp63α stabilization to promote cell migration in wound healing assay in vitro [28], suggesting that activation of YAP-ΔNp63α axis can facilitate cell

Table 1
A list of differentially expressed genes related to cell adhesion and cell motility.

Symbol	MST1KO/Ctl	MST2KO/Ctl
OCLN	0.04***	0.26***
CLDN1	0.02***	0.03***
F11R	0.38***	0.61***
MPZL2	0.39**	1.78**
DSP	0.26***	0.42***
JUP	0.22***	0.57***
CDH1	0.03***	0.33***
CDH3	0.15***	0.36***
ITGB4	0.67**	0.62**
ITGA4	0.90^{ns}	11.77**
ITGA7	1.00^{ns}	2.23*
COL4A1	0.76^{ns}	2.17**
COL4A4	0.67^{ns}	3.00**
COL6A2	2.13^{ns}	38.65**
COL9A3	0.75^{ns}	13.31**
ACTRT3	0.84^{ns}	2.36*
FLNC	0.36**	18.86**
MYLK2	3.67*	7.83*
RAC3	0.94^{ns}	3.09**
PARVB	0.94^{ns}	2.56***
SNAI1	1.63^{ns}	6.63**
SNAI2	1.70***	1.14^{ns}
TP63	0.39**	0.76**

Numbers indicate fold changes of expression.
***, $p < 0.001$; **, $p < 0.01$; *, $p < 0.05$; ns: not significant.

migration. The reason for discrepancy with our results is not clear.

The role of reactive oxygen species (ROS), including hydrogen peroxide (H_2O_2) and antioxidants, in cancer development is complex, because of their context-dependent ability to promote or suppress tumorigenesis. In this study, we show that elevated ROS by treatment of a moderate dose of H_2O_2 or piperlongumine can effectively inhibit cell mobility, through upregulation of ΔNp63α expression. Notably, consistent with our previously study that showed that oncogenic protein, including $KRas^{G12V}$ $p110\alpha^{H1047R}$ or Her2, inhibits the expression of ΔNp63α resulting in increased cell mobility [19], elevated ROS led to partial recovery of ΔNp63α expression thereby resulting in significant suppression of oncogene-induced cell migration. Thus, it is plausible that adequately elevated ROS levels in cancer cells may help to overcome activated oncogenic signaling in suppression of tumor development and that ΔNp63α is a critical effector in the oxidative stress signaling pathway.

Then, how does oxidative stress lead to upregulation of ΔNp63α? Thioredoxin-1 (Trx1), a conserved antioxidant protein with disulfide reductase activity, physically associates with the SARAH domain of MST1 thereby inhibiting the homodimerization and autophosphorylation of MST1 at Thr183, thus preventing MST1 activation. H_2O_2 abolishes this interaction and causes the activation of MST1 [36]. Indeed, we found that H_2O_2 or piperlongumine induces the phosphorylation and activation of MST1/2, which in turn promotes nuclear accumulation of FoxO3a, consistent with previous reports that activated MST1/2 can directly phosphorylate FoxO3a at S207 and affect nuclear accumulation [12]. Consistent with our previous study [19], nuclear FoxO3a can directly transactivate ΔNp63α gene expression, which in turn activates the expression of ITGB4 and impacts on cell mobility. Importantly, knockdown of MST2 effectively abolishes the oxidative stress-induced up-regulation of the FoxO3a/ΔNp63α/ITGB4 axis and inhibition of cell migration, indicating that the MST2-FoxO3a-ΔNp63α-ITGB4 axis is essential for oxidative stress signaling in cell mobility.

A important question is whether the Hippo kinases MST1/MST2 regulate cell migration through the key downstream YAP in response to oxidative stress, as it has been reported that the canonical Hippo pathway is involved in regulating metastasis [37,38]. Our results indicate that ablation of YAP significantly reduces ΔNp63α expression, consistent with previous reports that YAP can directly interact with and stabilize ΔNp63α protein [27,28]. However, our results show that ablation of YAP imposes only marginal effects on H_2O_2-induced upregulation of ΔNp63α and has little effects on oxidative stress-induced inhibition of cell migration. These results indicate that MST2 regulates cell migration and tumor metastasis, most likely independent of YAP in response to oxidative stress. However, it remains conceivable that YAP may directly or indirectly regulate cell migration and tumor metastasis in other ways.

Given the structural similarities, in which MST1 and MST2 are 74% identical overall and 94% identical within their catalytic domains at their N-terminuses, it is not surprising that MST1 and MST2 share many similar biological functions via the MST1/2-LAST1/2-YAP/TAZ pathway and are regulated in similar fashions in response to various extracellular signals. For example, single knockout mice are viable and do not exhibit either obvious abnormalities or organ overgrowth while simultaneous deletion of MST1 and MST2 results in embryonic lethality [39]. Regarding tumor development, double conditional MST1/2 knockout in mice promote tumorigenesis of the liver and intestines [40]. However, several studies indicate that MST1 and MST2 have distinctive functions. Whereas $MST1^{-/-}$ mice are viable and fertile with a reduced number of mature naïve T cells, $MST2^{-/-}$ mice exhibit no immunological detects. In addition, over a period of 18–24 months, 2/23 $MST1^{-/-}$ mice developed lethal histolytic sarcomas while 1/15 $MST2^{-/-}$ mice developed a mammary tumor [41]. Combined MST1/2 deficiency in the liver results in massive overgrowth and hepatocellular carcinoma (HCC). Re-expression of MST1, but not MST2, abrogates the tumorigenicity [41], indicating that MST1 has potent inhibitory functions in tumor initiation/growth.

At the cellular level, functional outputs are distinctively different following the ablation of MST1 or MST2. Ablation of MST1 leads to scattered cell growth but has no effects on cell migration, concomitant with down regulation of E-cadherin. Re-expression of E-cadherin completely abolishes scattering cell growth with apparently normal colony formation. By sharp contrast, ablation of MST2 results in increased cell migration with normal colony formation, concomitant with down regulation of ITGB4. Because both MST1 and MST2 target FoxO3a and ΔNp63α that critically regulates E-cadherin and ITGB4 gene transcription, how does MST1KO impact E-cadherin most strikingly while MST2KO impacts ITGB4 most significantly? A plausible possibility is that additional factor(s) is important in MST1-or MST2-mediated regulation of E-cadherin and ITGB4. In fact, our data show that MST2KO leads to downregulation of ITGB4 at both transcription and protein stability levels. Notably, FoxO3a can directly transactivate E-cadherin gene expression [42]. However, under our experimental settings, restoration of ΔNp63α effectively rescues ablation of FoxO3a-mediated downregulation of E-cadherin, indicating that the FoxO3a-ΔNp63α axis is most likely responsible for the regulation of E-cadherin.

The distinctive function of MST2 and MST1 in the regulation of cell mobility is further supported by the analyses of RNA-seq of MST1KO and MST2KO cells derived from the CRISPR/Cas9 system. Most strikingly, loss of MST1 significantly downregulates genes involved in cell-cell junction including E-cadherin, occludin, claudin1, JAM-1, desmoplakin and plakoglobins. By contrast, loss of MST2 significantly upregulates genes that facilitate cell migration, including genes involved cell-matrix adhesion (ITGA4, ITGB7, COL4A1, COL4A4, COL6A2, COL9A3) and cell skeleton organization (ACTRT3, FLNC, MYLK2).

Notably, MST1KO and MST2KO leads to significant upregulation of SNAI2 (SLUG) or SNAI1 (SNAIL), respectively, both of which are critical transcription factor promoting epithelial to mesenchymal transition (EMT) [43]. Our results indicate that MST2KO significantly downregulates integrin β4 expression. Several pieces of evidence support the notion that reduced integrin β4 expression promotes cell migration and is associated with tumor metastasis. Knockdown of integrin β4 promotes cell migration and effectively blocks H2O2-induced cell migration. In addition, reduced expression of integrin β4 is correlated with human breast carcinoma and in metastasized lung nodules derived from

MMTV-PyMT mice. Consistently, it has been reported that reduced ITGB4 expression promotes cancer cell migration [44]. However, high expression of integrin β4 appears to be important in driving breast cancer migration and metastasis [45]. The reasons for this discrepancy is unclear and deserves further investigation. It is conceivable that expression of integrin β4 is tightly controlled and the ultimate biological outcome is determined by various intra- and extra-signaling.

Together, these results strongly suggest that cancer-associated downregulation of MST1 and MST2 (both total and phosphorylated MST1/MST2 protein levels), which results in EMT, disruption of cell-cell junction and alteration of cell-matrix adhesion at the cellular levels, may contribute to tumor metastasis during cancer development. In particular, these results demonstrate that oxidative stress inhibits cell migration and tumor metastasis via a noncanonical Hippo pathway involved in MST2-FoxO3a-ΔNp63α axis (Fig. 6c).

Acknowledgements

We thank faculty and members of CGMA for helpful discussions and for Mr. Han Kang for help on instruments. This work was supported by National Natural Science Foundation of China (81802951) to Y.Y; National Key R&D Program of China (2018YFC2000100), National Natural Science Foundation of China (81520108020, 81830108, 81861148031 and 81330054) and Sichuan Department of Science and Technology International Cooperation and Exchange Program (2017HH0057) to Z-X X.

Appendix A. Supplementary data

Supplementary data to this article can be found online at https://doi.org/10.1016/j.redox.2019.101233.

References

[1] D. Trachootham, J. Alexandre, P. Huang, Targeting cancer cells by ROS-mediated mechanisms: a radical therapeutic approach? Nat. Rev. Drug Discov. 8 (7) (2009) 579–591.
[2] C. Gorrini, I.S. Harris, T.W. Mak, Modulation of oxidative stress as an anticancer strategy, Nat. Rev. Drug Discov. 12 (12) (2013) 931–947.
[3] B.C. Dickinson, C.J. Chang, Chemistry and biology of reactive oxygen species in signaling or stress responses, Nat. Chem. Biol. 7 (8) (2011) 504–511.
[4] Y.J. Liao, H.Y. Bai, Z.H. Li, J. Zou, J.W. Chen, F. Zheng, et al., Longikaurin A, a natural ent-kaurane, induces G2/M phase arrest via downregulation of Skp2 and apoptosis induction through ROS/JNK/c-Jun pathway in hepatocellular carcinoma cells, Cell Death Dis. 5 (2014) e1137.
[5] M.S. Schieber, N.S. Chandel, ROS links glucose metabolism to breast cancer stem cell and EMT phenotype, Cancer Cell 23 (3) (2013) 265–267.
[6] E. Piskounova, M. Agathocleous, M.M. Murphy, Z. Hu, S.E. Huddlestun, Z. Zhao, et al., Oxidative stress inhibits distant metastasis by human melanoma cells, Nature 527 (7577) (2015) 186–191.
[7] P. Karpowicz, J. Perez, N. Perrimon, The Hippo tumor suppressor pathway regulates intestinal stem cell regeneration, Development 137 (24) (2010) 4135–4145.
[8] B. Zhao, L. Li, Q. Lei, K.L. Guan, The Hippo-YAP pathway in organ size control and tumorigenesis: an updated version, Genes Dev. 24 (9) (2010) 862–874.
[9] X. Du, J. Wen, Y. Wang, P.W.F. Karmaus, A. Khatamian, H. Tan, et al., Hippo/Mst signalling couples metabolic state and immune function of CD8alpha(+) dendritic cells, Nature 558 (7708) (2018) 141–145.
[10] B.Z. K T, K.L. G, The Hippo pathway in organ size control, tissue regeneration and stem cell self-renewal, Nat. Cell Biol. 13 (8) (2011) 877–883.
[11] Q. Lei, H. Zhang, B. Zhao, Z. Zha, F. Bai, X. Pei, et al., TAZ promotes cell proliferation and epithelial-mesenchymal transition and is inhibited by the Hippo pathway, Mol. Cell. Biol. 28 (7) (2008) 2426.
[12] M.K. Lehtinen, Z. Yuan, P.R. Boag, Y. Yang, J. Villen, E.B. Becker, et al., A conserved MST-FOXO signaling pathway mediates oxidative-stress responses and extends life span, Cell 125 (5) (2006) 987–1001.
[13] Z. Yuan, M.K. Lehtinen, P. Merlo, J. Villen, S. Gygi, A. Bonni, Regulation of neuronal cell death by MST1-FOXO1 signaling, J. Biol. Chem. 284 (17) (2009) 11285–11292.
[14] E. Candi, A. Rufini, A. Terrinoni, D. Dinsdale, M. Ranalli, A. Paradisi, et al., Differential roles of p63 isoforms in epidermal development: selective genetic complementation in p63 null mice, Cell Death Differ. 13 (6) (2006) 1037–1047.
[15] G.X. Wang, H.C. Tu, Y. Dong, A.J. Skanderup, Y. Wang, S. Takeda, et al., DeltaNp63 inhibits oxidative stress-induced cell death, including ferroptosis, and cooperates with the BCL-2 family to promote clonogenic survival, Cell Rep. 21 (10) (2017) 2926–2939.
[16] A. Latina, G. Viticchie, A.M. Lena, M.C. Piro, M. Annicchiarico-Petruzzelli, G. Melino, et al., DeltaNp63 targets cytoglobin to inhibit oxidative stress-induced apoptosis in keratinocytes and lung cancer, Oncogene 35 (12) (2016) 1493–1503.
[17] J. Bergholz, Z.X. Xiao, Role of p63 in development, tumorigenesis and cancer progression, Cancer Microenvironment 5 (3) (2012) 311–322.
[18] D.K. Carroll, J.S. Carroll, C.O. Leong, F. Cheng, M. Brown, A.A. Mills, et al., p63 regulates an adhesion programme and cell survival in epithelial cells, Nat. Cell Biol. 8 (6) (2006) 551–561.
[19] L. Hu, S. Liang, H. Chen, T. Lv, J. Wu, D. Chen, et al., DeltaNp63alpha is a common inhibitory target in oncogenic PI3K/Ras/Her2-induced cell motility and tumor metastasis, Proc. Natl. Acad. Sci. U. S. A. 114 (20) (2017) E3964–E3973.
[20] W.D. Tilley, S.S. Lim-Tio, D.J. Horsfall, J.O. Aspinall, V.R. Marshall, J.M. Skinner, Detection of discrete androgen receptor epitopes in prostate cancer by immunostaining: measurement by color video image analysis, Cancer Res. 54 (15) (1994) 4096–4102.
[21] W. Sun, J. Bao, W. Lin, H. Gao, W. Zhao, Q. Zhang, et al., 2-Methoxy-6-acetyl-7-methyljuglone (MAM), a natural naphthoquinone, induces NO-dependent apoptosis and necroptosis by H2O2-dependent JNK activation in cancer cells, Free Radic. Biol. Med. 92 (2016) 61–77.
[22] H. Dhillon, S. Chikara, K.M. Reindl, Piperlongumine induces pancreatic cancer cell death by enhancing reactive oxygen species and DNA damage, Toxicol Rep 1 (2014) 309–318.
[23] S. Thongsom, W. Suginta, K.J. Lee, H. Choe, C. Talabnin, Piperlongumine induces G2/M phase arrest and apoptosis in cholangiocarcinoma cells through the ROS-JNK-ERK signaling pathway, Apoptosis 22 (11) (2017) 1473–1484.
[24] Y. Samuels, Z. Wang, A. Bardelli, N. Silliman, J. Ptak, S. Szabo, et al., High frequency of mutations of the PIK3CA gene in human cancers, Science 304 (5670) (2004) 554-554.
[25] M.R. Ramsey, N.E. Sharpless, ROS as a tumour suppressor? Nat. Cell Biol. 8 (11) (2006) 1213–1215.
[26] B. Mao, Y. Gao, Y. Bai, Z. Yuan, Hippo signaling in stress response and homeostasis maintenance, Acta Biochim. Biophys. Sin. 47 (1) (2015) 2–9.
[27] M. Yuan, P. Luong, C. Hudson, K. Gudmundsdottir, S. Basu, c-Abl phosphorylation of ΔNp63α is critical for cell viability, Cell Death Dis. 1 (1) (2010) e16.
[28] M.L. Fisher, C. Kerr, G. Adhikary, D. Grun, W. Xu, J.W. Keillor, et al., Transglutaminase interaction with α6/β4-integrin stimulates YAP1-dependent ΔNp63α stabilization and leads to enhanced cancer stem cell survival and tumor formation, Cancer Res. 76 (24) (2016) 7265–7276.
[29] A. Delaunay, D. Pflieger, M.-B. Barrault, J. Vinh, M.B. Toledano, A thiol peroxidase is an H2O2 receptor and redox-transducer in gene activation, Cell 111 (4) (2002) 471–481.
[30] P.A.J. Muller, A.G. Trinidad, P. Timpson, J.P. Morton, S. Zanivan, P.V.E. van den Berghe, et al., Mutant p53 enhances MET trafficking and signalling to drive cell scattering and invasion, Oncogene 32 (10) (2012) 1252–1265.
[31] C.T. Guy, R.D. Cardiff, W.J. Muller, Induction ofMammaryTumorsbyExpression ofPolyomavirus middle T oncogene: a transgenic MouseModel for Metastatic disease, Mol. Cell. Biol. 12 (3) (1992) 954–961.
[32] J. Bergholz, Y. Zhang, J. Wu, L. Meng, E.M. Walsh, A. Rai, et al., ΔNp63α regulates Erk signaling via MKP3 to inhibit cancer metastasis, Oncogene 33 (2) (2014) 212.
[33] F. Wang, L. Wang, J. Pan, PACE4 regulates proliferation, migration and invasion in human breast cancer MDA-MB-231 cells, Mol. Med. Rep. 11 (1) (2015) 698.
[34] C.E. Barbieri, L.J. Tang, K.A. Brown, J.A. Pietenpol, Loss of p63 leads to increased cell migration and up-regulation of genes involved in invasion and metastasis, Cancer Res. 66 (15) (2006) 7589–7597.
[35] H. Fukushima, F. Koga, S. Kawakami, Y. Fujii, S. Yoshida, E. Ratovitski, et al., Loss of ΔNp63α promotes invasion of urothelial carcinomas via N-cadherin/Src homology and collagen/extracellular signal-regulated kinase pathway, Cancer Res. 69 (24) (2009) 9263–9270.
[36] J.S. Chae, S. Gil Hwang, D.S. Lim, E.J. Choi, Thioredoxin-1 functions as a molecular switch regulating the oxidative stress-induced activation of MST1, Free Radic. Biol. Med. 53 (12) (2012) 2335–2343.
[37] D. Chen, Y. Sun, Y. Wei, P. Zhang, A.H. Rezaeian, J. Teruya-Feldstein, et al., LIFR is a breast cancer metastasis suppressor upstream of the Hippo-YAP pathway and a prognostic marker, Nat. Med. 18 (10) (2012) 1511–1517.
[38] C.-W. Lin, Y.-L. Chang, Y.-C. Chang, J.-C. Lin, C.-C. Chen, S.-H. Pan, et al., MicroRNA-135b Promotes Lung Cancer Metastasis by Regulating Multiple Targets in the Hippo Pathway and LZTS1 vol. 4, (2013).
[39] D. Zhou, C. Conrad, F. Xia, J.S. Park, B. Payer, Y. Yin, et al., Mst1 and Mst2 maintain hepatocyte quiescence and suppress hepatocellular carcinoma development through inactivation of the Yap1 oncogene, Cancer Cell 16 (5) (2009) 425–438.
[40] F. Qin, J. Tian, D. Zhou, L. Chen, Mst1 and Mst2 kinases: regulations and diseases, Cell Biosci. 3 (1) (2013) 31.
[41] D. Zhou, C. Conrad, F. Xia, J.S. Park, B. Payer, Y. Yin, et al., Mst1 and Mst2 maintain hepatocyte quiescence and suppress hepatocellular carcinoma development through inactivation of the Yap1 oncogene, Cancer Cell 16 (5) (2009) 425–438.
[42] C.C. Chou, K.H. Lee, I.L. Lai, D. Wang, X. Mo, S.K. Kulp, et al., AMPK reverses the mesenchymal phenotype of cancer cells by targeting the Akt-MDM2-Foxo3a signaling axis, Cancer Res. 74 (17) (2014) 4783–4795.
[43] C. Kudo-Saito, H. Shirako, T. Takeuchi, Y. Kawakami, Cancer metastasis is accelerated through immunosuppression during snail-induced EMT of cancer cells, Cancer Cell 15 (3) (2009) 195–206.
[44] A. Ferraro, C.K. Kontos, T. Boni, I. Bantounas, D. Siakouli, V. Kosmidou, et al., Epigenetic regulation of miR-21 in colorectal cancer: ITGB4 as a novel miR-21 target and a three-gene network (miR-21-ITGB4-PDCD4) as predictor of metastatic tumor potential, Epigenetics 9 (1) (2014) 129–141.
[45] K. Vuoriluoto, H. Haugen, S. Kiviluoto, J.P. Mpindi, J. Nevo, C. Gjerdrum, et al., Vimentin regulates EMT induction by Slug and oncogenic H-Ras and migration by governing Axl expression in breast cancer, Oncogene 30 (12) (2011) 1436–1448.